Discover Applied Sciences

Research

Functionalized nanoparticles-based surface treatment as an alternative to mitigate deterioration in fired clay materials

D. Cruz-Moreno[1] · M. Neri-Álvarez[1] · G. Ortiz-Rabell[1] · M. A. Neri-Flores[2] · G. Fajardo-San-Miguel[1]

Received: 22 November 2024 / Accepted: 3 April 2025
Published online: 24 April 2025

Abstract
The preservation of built and cultural heritage poses numerous challenges globally, given its intrinsic value and historical significance. This study assesses the performance of two surface treatments, comprising a dispersion of functionalized silicon-based nanoparticles at a concentration of 0.1% in water. Two different variants were examined: the first being simple functionalized (NS) "T1" and the second being dehydrated functionalized (NF) "T2" nanoparticles. The application of both treatments, T1 and T2, was carried out on specimens of fired clay tile using a sponge brush in two layers, with 30 min between each layer. These treatments were compared with the application of three commercial products: a 90% siloxane-based reactive grade compound (SX), a solvent-based silicone resin active (C1), and silicone-based active and water-conveyed additives (C2). After application, the specimens were evaluated simultaneously to determine the behavior and effectiveness of the treatments in two different exposure environments (in a natural urban/industrial environment for 24 months and a controlled environment in a QUV chamber for 2000 h). The performance of the treatment was assessed through the measurement of static contact angle, capillary water absorption, and optical appearance in accordance with colorimetric and FTIR standards. It was established that the application of the T2 treatment yields comprehensive outcomes in fired clay tiles as a hydrophobic treatment, imparting advantageous properties. Urban and industrial settings significantly impact visual aesthetics, as reflected in high ΔE* values. Functionalized nanoparticles demonstrate enhanced performance even at low concentrations, making them ideal for preserving the aesthetics and structural integrity of walls and roof tiles in heritage buildings.

Article Highlights

- Dehydration of the nanoparticle favors the delay of hydroxylation.
- T2 presents a high resistance to weathering and stability to the substrate.
- T2 reduced the absorption rate to two orders of magnitude, increasing its durability.
- The effectiveness of T2 is guaranteed with a contact angle > 90º and ΔE* < 5.

Keywords Clay roof tiles · Surface treatment · Weathering · Preventive conservation · Durability

✉ G. Fajardo-San-Miguel, gerardo.fajardosn@uanl.edu.mx; D. Cruz-Moreno, dulce.cruzmrn@uanl.edu.mx; M. Neri-Álvarez, monica.nerialvr@uanl.edu.mx; G. Ortiz-Rabell, GORTIZRL@uanl.edu.mx; M. A. Neri-Flores, miguel.neri@cimav.edu.mx |
[1]Universidad Autónoma de Nuevo León, Facultad de Ingeniería Civil, UANL – FIC, Av. Universidad S/N, Ciudad Universitaria, San Nicolás de los Garza, Nuevo León 66455, México. [2]Centro de Investigación en Materiales Avanzados, CIMAV, S.C., Chihuahua, Chih., Mexico.

1 Introduction

The preservation of modern and ancient architectural heritage is crucial for maintaining social and cultural roots. It is the responsibility of each country to protect and maintain its heritage from deterioration [1]. Heritage includes both contemporary and historical elements, and it serves as an important and tangible resource for nations [2, 3]. Therefore, agencies responsible for heritage management and preservation are highly interested in its conservation and durability [4]. On the other hand, the combined effects of pollution and global climate change have consistently damaged clay, limestone, and other stone-based constructions materials, whether contemporary or historical. The main deterioration mechanisms typically start with the interaction of the medium with the surface of materials, also known as substrates [5–8]. While various methods have been utilized to conserve these materials, they often lack durability and efficiency [9]. In recent decades, the focus has shifted towards developing alternative conservation methods for clay tiles and materials, particularly in European and Asian countries. This is especially pertinent as approximately 90% of the historical heritage in these regions is comprised of clay tiles [8, 9]. Mexico holds a significant architectural legacy, with 35 UNESCO World Heritage Sites, including over 10 historic centers of vice-regal cities. These cities are characterized by extensive infrastructure adorned with clay tiles, commonly known as Spanish tiles. Thus, a key objective of this research is to develop a treatment for creating durable clay tile surfaces for ancient and modern heritage and new construction conservation. Most of the technologies currently available for the conservation and restoration of heritage are complex and rely on biological, chemical, and physical treatments [10]. It is crucial to carefully manage environmental parameters such as physical conditions, temperature, and humidity, as sudden changes can have a detrimental impact on the durability of materials [4, 11]. Such changes have the potential to cause deterioration, which may result in the partial or complete loss of important historical and cultural heritage. These alterations have the potential to result in the degradation of both modern and ancient architectural heritage, potentially leading to their partial or complete loss. Furthermore, it is anticipated that heritage sites of all kinds will be at risk in a shifting climate, facing numerous unforeseen challenges. As a result, innovative solutions are being devised to ensure their protection [12]. A wide range of surface treatments are currently used to provide hydrophobic and biocidal properties, offering commercial protective effects [11, 13]. However, these products are mainly designed to preserve cement and stone-based materials, resulting in limited performance due to the disadvantages associated with the substrate they are applied to, such as porosity, surface roughness, and pH. As a result, the most common solutions involve creating physical and chemical barriers through specific treatments based on binders or crystallizers. All forms of built heritage are susceptible to gradual deterioration in their component materials (such as stones, mortars, and clays) due to environmental factors. These factors include the accumulation of salts and metals, the presence of water vapor, and the cyclical impact of high temperatures and humidity [1, 12, 14].

All built heritage faces problems of progressive deterioration in its constituent materials (rocks, mortars, clays, among others) that are caused by environmental factors such as the concentration of salts, metals, water vapor, cyclical effects of high temperature and humidity, etc. [1, 12, 14]. The literature reports various degradation factors and alterations that can damage clay tiles. For instance, a study by Hosseini et al., 2018, identified water as the primary factor contributing to degradation in ornamental masonry. Water serves as a transport medium for biological, physical, and chemical agents, which can have a combined and synergistic effect on the material [15]. There are different types of deterioration, such as biodeterioration caused by living organisms. When porous materials are in contact with water or saturated soil, various ions can easily enter the material, leading to unwanted changes in its physical and chemical properties. Additionally, chemicals like acids, alkalis, gases, oils, fats, and sugars can cause chemical corrosion. The accumulation of biogenic substances due to the intensive growth of microorganisms further contributes to deterioration. Thermal factors also play a role, with water acting as a thermal conductor that accumulates and wets masonry units, thereby increasing thermal dispersion.

The rise in temperature from solar radiation can hasten the breakdown of materials by accelerating chemical reactions, especially when combined with humidity. This acceleration can lead to increased solubility and dissociation of salts, acids, and bases, as well as a decrease in viscosity and an increase in ion mobility within the materials. For instance, aggressive atmospheric agents like sulfur dioxide or carbonic acid can interact with calcareous binders, such as lime and calcium carbonate, making them more soluble and leading to the rapid deterioration of masonry [16]. Additionally, temperature fluctuations, whether gradual or sudden, can induce stress through differential thermal expansion, resulting in cracking. Fired clay tiles, for example, may expand when wet, depending on their porosity and surface characteristics, affecting the extent of water penetration. UV light also has a significant impact on the

degradation of materials. Sunlight contains photons with energies ranging from 0.5 eV to 4 eV, with about 5% of the energy in the form of ultraviolet photons exceeding 3 eV. These high-energy photons have the ability to break chemical bonds, contributing to material deterioration. Additionally, the increase in temperature on roofs resulting from solar radiation absorption is detrimental to the longevity of materials. Furthermore, air pollution introduces salts that lead to efflorescence, manifesting as a soluble white powder on the surface of coatings [17]. Over time, these salts accumulate within porous materials and, when combined with water, migrate in various directions within the material. Ultimately, crystallized salts tend to accumulate in areas where water evaporates [18]. Gases, combined with rainwater, condensation, temperature, humidity, aerosols, and environmental agents, play a significant role in the dispersion and deposition of pollutants [19]. The level of relative humidity then influences the adsorption of substances and their interaction with material components. Additionally, the physical structure can undergo changes due to growth within the material, leading to cracking, disaggregation, or increased volume. Furthermore, contamination is a key source of deposition films that result in dirt stains on building facades [20]. As a result, the current focus in addressing these issues in clay-based masonry involves developing innovative treatments to mitigate deterioration and transform them into advanced materials.

The treatments in this context must adhere to the requirements set by management and preservation agencies, while also meeting the current market demands for unique products with multifunctional properties. It has been observed that surface treatments incorporating nanomaterials can effectively reduce degradation through physical, chemical, and biological means, as they offer multiple properties such as self-cleaning [20, 21], bactericidal effects [22, 23], superhydrophobicity [24, 25], anti-fog properties [25, 26], omniphobic characteristics [27, 28], and more.

In order to minimize changes to the aesthetic appearance of historical or current heritage substrates, interventions on materials must adhere to specific criteria. These criteria dictate that the total color differential (ΔE^*) of the substrate should be minimal, with a specified limit of $\Delta E^* < 2$, or where appropriate, $\Delta E^* < 10$, as outlined in EN 16581:2016 and ISO 12647–4 [29]. Numerous studies have explored the use of TiO_2, SiO_2, and Al_2O_3-based nanomaterials for this purpose. For instance, S. Borhani-Esfahani et al. [30] have developed silicon-based nanoparticles utilizing organically modified silicate (ormosil) as a matrix and titanium-silica nanoparticles as a reinforcing phase to protect the tile facades of historical buildings. These efforts aim to balance the need for conservation and maintenance with the imperative to minimize visual alterations to the heritage substrates.

The study findings demonstrate that a clear hydrophobic coating can be attained by incorporating up to 20% by weight of PDMS-OH into the initial sols, without the need for additional solvents or highly toxic catalysts. For an environmentally friendly, transparent, hydrophobic, and UV-absorbing nanocomposite coating, the ideal composition may consist of 20% by weight of PDMS-OH and approximately 0.025% by weight of silica-titanium core–shell nanoparticles. In a related study, Maria Kouroutzi et al. [31] investigated the use of TiO_2 nanoparticles in the production of clay tiles. Their experiments involved three types of TiO_2 nanoparticles, with and without polyethylene glycol (PEG). These ceramic tiles underwent a dip coating process to achieve the desired photocatalytic surface, leading to an increase in surface areas and potentially enhancing the photocatalytic efficiency.

The use of nanoparticles in this context offers several benefits, such as reducing cracking, improving hydrophobicity through increased surface roughness, enhancing resistance to weathering, and providing good stability and interaction with the substrate [31]. Ferri et al. studied the wide-ranging potential of titanium nanoparticles in architectural preservation, thanks to their photocatalytic activity that aids in breaking down organic pollutants and creating self-cleaning properties on surfaces [32]. Furthermore, Kapridaki et al. developed a SiO_2-TiO_2 nanocomposite coating using TEOS, PDMS-OH, and titanium isopropoxide (TTIP) as a precursor for monument conservation [33]. Liu et al. have successfully developed a hydrophobic and transparent nanocomposite coating that possesses self-cleaning capabilities [34]. Their research has inspired further exploration into the use of silicon nanoparticles to improve the longevity of clay roof tiles in Mexican viceregal heritage. Traditional surface treatments, such as siloxanes, silanes, acrylics, and resins, have been found to struggle with maintaining stability in cement-based matrices due to their high alkalinity and susceptibility to weathering. As a solution, hybridization or functionalization of existing materials has emerged as a promising approach to enhance or restore hydrophobic properties, providing excellent thermal stability, resistance to weathering, low surface energies, and prolonged durability [35–37]. The exceptional thermal stability, resistance to weathering, and low surface energies of these materials contribute to their prolonged durability. However, the stability and durability of functionalized nanoparticles rely heavily on the type of surface modifier (organic or inorganic) used for their functionalization, as well as the nature of the modification, whether it is physical or chemical. Current products are constrained by the combined effects of physical, chemical, and environmental factors, prompting the exploration of sustainable and effective alternatives to enhance protection [8]. Other articles found in the literature as a protective tool

for cultural heritage application has developing a simple and low-cost synthesis route for creating superhydrophobic surfaces on stones and other building materials [38–41].

Therefore, it is essential to thoroughly analyze the physical and chemical characteristics of both the functionalized nanoparticles and the substrate in order to develop a surface treatment that can effectively withstand weathering. Understanding their combined interaction and the stability-durability relationship is crucial. This approach not only extends the service life of the substrate but also reduces the necessity for premature intervention, ultimately promoting sustainable consumption and minimizing environmental impact.

This study evaluates two treatment alternatives using functionalized nanoparticles to modify the surface of fired clay tiles, aiming to provide multifunctional properties for the conservation of heritage buildings. These methods offer easily applicable solutions to preserve architectural and historical details, while also enhancing resistance to deterioration. The research aims to address the current challenge of conserving Mexican architectural heritage, particularly the widespread use of clay tiles in roofing infrastructure across the country, including areas of historical significance and numerous towns.

2 Materials and methods

2.1 Nanoparticle synthesis

Two types of nanoparticles were assessed: "T1" and "T2". The "T1" nanoparticles were functionalized in a simple manner, while the "T2" nanoparticles were functionalized after dehydration. These correspond to NS and NF, respectively, and were produced using the sol–gel method, following the synthesis procedure outlined in a previous study [35, 42].

The synthesis process involved the use of tetraethyl orthosilicate (TEOS) as the silica precursor, with ethyl alcohol as the solvent, deionized water, and ammonium hydroxide as the catalyst. To functionalize the NS, 1,1,3,3-tetramethyldisiloxane was used as the surface modifier, while nitric acid acted as the dehydrating agent. Initially, ethyl alcohol was vigorously stirred at 70 °C, and then TEOS was added while maintaining the temperature and stirring for 30 min. Subsequently, ammonium hydroxide was introduced and allowed to react for another 30 min before slowly adding water and continuing the reaction for an additional 60 min. Excess ammonium hydroxide was added dropwise until a clear gel formed, which was then placed in an oven at 110 °C for 24 h to evaporate excess solvent and water.

During the synthesis of NF, the functionalization process commenced with the addition of distilled water during the NS sol–gel synthesis, and continued for a 60-min reaction period. Subsequently, 1,1,3,3-tetramethyldisiloxane was introduced and allowed to react for 120 min. Nitric acid was then added for dehydration and surface modification. Finally, carefully adding dropwise, ammonium hydroxide was allowed to react for 24 h before placing the product in an oven at 110 °C for another 24 h.

2.2 Preparation of specimens

In this study, we utilized commercial Portuguese tiles made entirely of fired clay, with dimensions of 40.5 × 25 cm (refer to Fig. 1**a**). The flat part of the tiles was sectioned into specimens measuring 4 × 4 cm, and a study area of 2.7 × 2.7 cm was delimited within this section (see Fig. 1**b**). The remaining part of the tile was covered with commercial waterproofing and sealant products. The specimens under study were subjected to the weather conditions of the Monterrey, Mex., metropolitan area beginning on November 17, 2017. The specimens samples were placed in an aluminum structure at a 45° angle facing south, in accordance with the ASTM D1435 – 13 standard (see Fig. 1**c**). About 6 specimens were prepared for each group under evaluation. This angle closely approximated the typical 35° inclination for roof placement.

2.3 Surface preparation of specimens

The specimens have been subjected to a surface area cleaning in accordance with the procedure outlined in the technical data sheet for the relevant commercial surface products. The cleaning process involved the use of tap water, a soft bristle brush, and absorbent paper. It is important to note that the samples used are from newly acquired tiles and do not exhibit any pathological issues resulting from weathering.

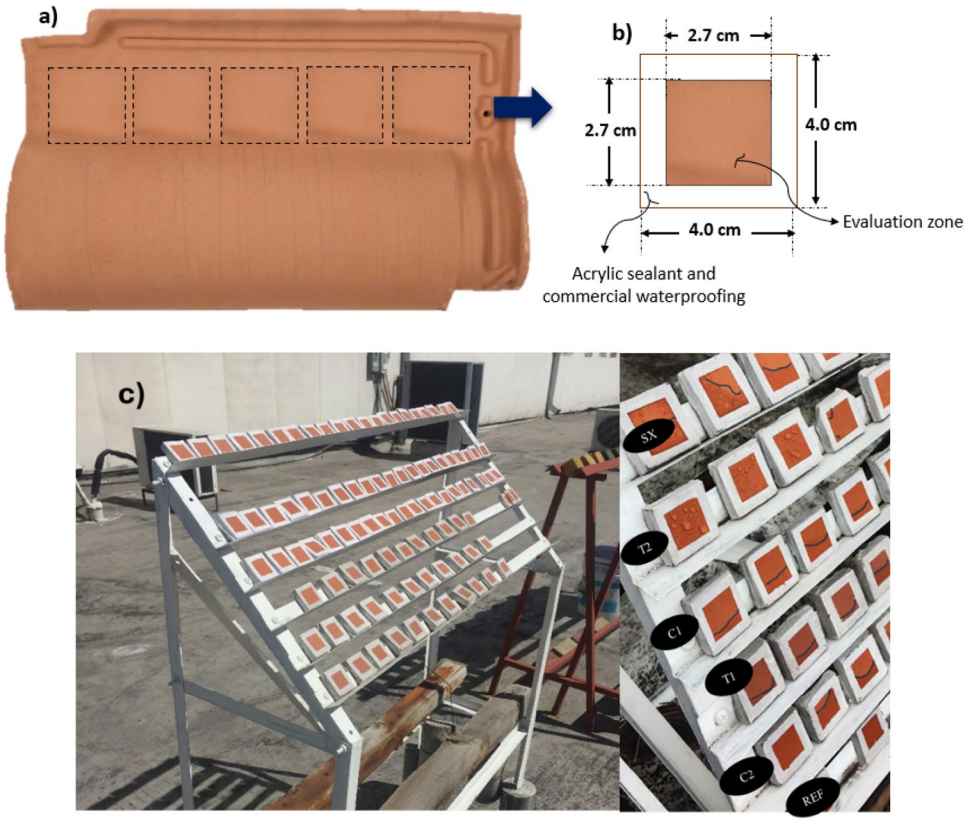

Fig. 1 **a** Commercial tiles, **b** specimens obtained for evaluation and **c** set-up for exposure

Table 1 Description of the surface treatments applied

ID	Description of the treatment
REF	Reference or specimen without treatment
C1	Commercial product with an active base of silicone resin, conveyed in a solvent, applied with a brush in two layers (as recommended in the technical sheet). C1 presented a colorless liquid consistency with a yield of 0.5 to 0.7 L/m^2 for two layers
C2	Commercial product with silicone-based actives and additives, conveyed in water, applied with a brush in two layers (recommended in the technical sheet). C2 presented a slightly milky liquid consistency with a yield between 0.5 to 0.6 in two layers
SX	The reagent consists of 90% siloxane base actives, specifically $[(CH_3)_2SiH]_2O$ from Sigma-Aldrich with a purity of 97%. It should be applied using a brush in two layers, with a 30-min interval between each layer for optimal results. SX presented a milky liquid consistency with a yield between 1.0 to 1.1 in two layers.
T1	Surface treatment is based on functionalized nanoparticles dispersed in water and applied with a brush in two layers, with a 30-min interval between each layer. T1 presented a slightly milky liquid consistency with a yield between 0.6 to 0.7 in two layers
T2	Surface treatment is based on dehydrated functionalized nanoparticles in water and applied with a brush in two layers, with a 30-min interval between each layer. T2 presented a slightly milky liquid consistency with a yield between 0.6 to 0.7 in two layers

2.4 Application of surface treatment

Table 1 provides a description of various surface treatments and their corresponding identification (ID) nomenclature. The commercial products (C1, C2, and SX) were administered to the clay samples using a polyurethane foam brush in two layers, in accordance with the technical sheet of manufacturers. It is important to note that for the nanoparticle-based products (T1 and T2), the application involved two layers, fully saturating the surface with a 30-min interval between each layer's application.

After the surface treatments were applied, the samples were carefully protected from the weather for a period of 48 h before being exposed to various media.

2.5 Aging procedure

In order to assess the performance of surface treatments in different environments, two weathering methods were employed. The first method involved exposure to natural environmental conditions, allowing for the evaluation of the treatments' behavior in real-world scenarios. The second method consisted of subjecting the treatments to controlled artificial conditions in a laboratory setting, known as accelerated weathering.

2.5.1 Urban/industrial environment

The durability and stability of various surface treatments in the presence of atmospheric pollutants were evaluated through natural exposure in an urban/industrial environment. Following the procedure outlined in ASTM D1435, a series of specimens were placed outdoors and marked with identifying numbers or symbols for easy identification after exposure. The specimens were marked on the non-exposed side to ensure visibility after advanced weathering. Initial appearance and physical-property data relevant to the evaluation method were recorded. The exposure area was located on the outer roof of the Institute of Civil Engineering (IIC-UANL) of the UANL in San Nicolás de Los Garza, Nuevo León, Mexico over a period of 24 months.

2.5.2 Accelerated weathering in UV chamber

The stability of the hydrophobic properties was assessed by subjecting the samples to accelerated aging cycles in an Accelerated Weathering Tester model QUV chamber, following the guidelines of ASTM G 151. The cycles involved alternating periods of 8 h at 60 °C with an irradiance of 1.55 W/m^2 (dry cycle) and 4 h at 50 °C with humidity (wet cycle), totaling 2000 h. This simulation aimed to replicate the effects of UV rays from sunlight on surface treatments in a laboratory setting.

2.6 Evaluation of treatment performance

An assessment of the performance and stability of the applied treatments was conducted through a physicochemical evaluation of the surface of the clay tile samples. It is important to note that samples were collected at various time points, including 3, 6, and 24 months for urban/industrial environment, as well as at 500 h, 1000 h, and 2000 h for an accelerated weathering. This approach allowed for a comprehensive understanding of the effects of the treatments over time, both in real-world conditions and under accelerated testing.

2.6.1 Visual appearance according to colorimetric standards

The evaluation of the optical appearance was conducted using the total color difference (ΔE*) technique, as per Eq. 1. The Datacolor CHECK equipment was utilized for this purpose, following the procedure outlined in ASTM D2244. The interpretation of results was carried out in accordance with standards EN 16581:2016 and ISO 12647–4.

$$\Delta E^* = \sqrt{\Delta L^{*2} + \Delta a^{*2} + \Delta b^{*2}} \quad (1)$$

where:

ΔE* = total color difference.
ΔL* = difference in light and dark (+ = brighter, − = darker).
Δa* = difference in red and green (+ = redder, − = greener).
Δb* = difference in yellow and blue (+ = more yellow, − = bluer).
L*, a*, and b* are the standard coordinates of the CIELab color space 1976 scale.

In order to illustrate the color differences, a simulation utilizing color modeling was carried out by inputting the color coordinates (L*, a*, and b*) into the NIX Color Sensor computer program. The input and output parameters were configured to correspond with the reference angle and illumination at D65/10° (values specified in CIELab).

2.6.2 Determination of hydrophobicity

The hydrophobic properties of the sample surfaces were evaluated using a goniometer model DSA25 (Drop Shape Analyzer) KRÜSS, in accordance with the ASTM D7334 standard. The measurements were conducted at 23 ± 2 °C and with a RH of ≥ 50%, using a drop volume of 6 µL. The contact angle between the liquid and the specimen surface was determined using the ADVANCE software version 1.9.2.3.

2.6.3 Measurement of capillary water absorption

The water absorption rate was determined in accordance with the procedure outlined in ASTM C 1585. Three specimens were chosen for each treatment and were initially dried before being coated with a waterproofing agent and an acrylic sealant to define the study area.

2.6.4 Fourier transform infrared spectrometry (FTIR)

The determination of the functional groups responsible for imparting hydrophobic properties to the surface of the exposed tiles during the experimental procedure was carried out using a Thermo Electron Nicolet 380 equipment, which operates within a frequency range of 500–4000 cm^{-1}. To achieve this, the treated section of the tile underwent mechanical roughening, and the resulting powders were subsequently dried at 60 °C for a period of 24 h.

2.7 Climatic data

In Mexico, the climate provides ideal conditions for the deterioration of ornamental masonry, particularly in warm humid and warm subhumid areas. These climates facilitate the access of pollutants and the growth of microorganisms, leading to accelerated deterioration of construction materials. The hot humid climate, covering 4.7% of the territory, is characterized by average annual temperatures between 22° and 26 °C, and annual rainfall between 2,000 and 4,000 mm. Meanwhile, the warm subhumid climate, covering 23% of the country, experiences annual rainfall between 1,000 and 2,000 mm and temperatures ranging from 22° to 26 °C, occasionally exceeding 26 °C in certain areas (data sourced from INEGI 2018) (Fig. 2).

The solar irradiation map of Mexico, as depicted in Fig. 3, indicates an annual average of 5.3 kWh/m^2 (5300 Wh/m^2) per day. In order to accelerate the degradation of the material, an accelerated exposure at 1.55 W/m^2 (0.0016 kW/m^2) was employed, surpassing the natural radiation levels.

The average variation of temperature, RH, rainfall, and UV index during the exposure period of the specimens is depicted in Fig. 4.

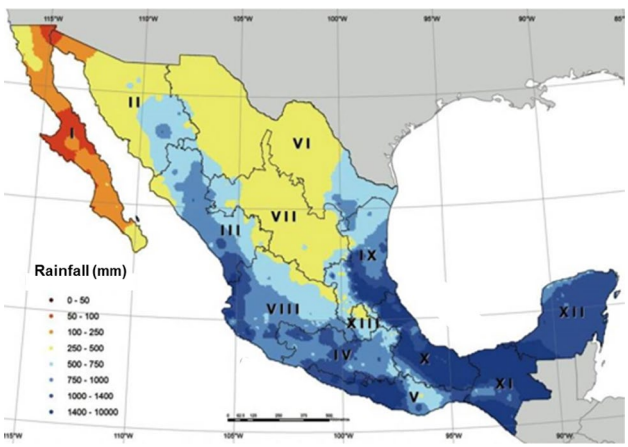

Fig. 2 Rainfall distribution in Mexico (INEGI; https://www.inegi.org.mx/temas/climatologia/)

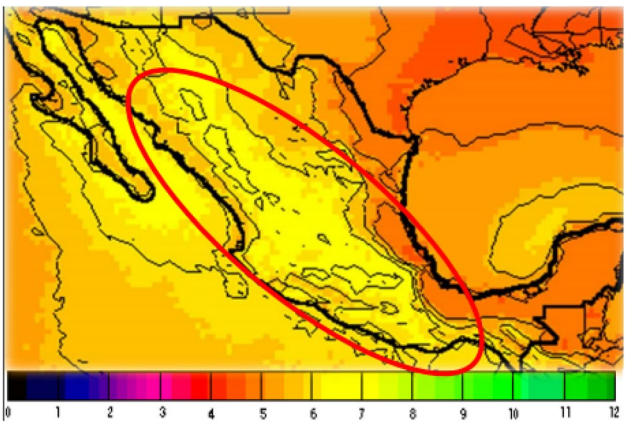

Fig. 3 Solar irradiance in Mexico (https://www.gob.mx/conagua)

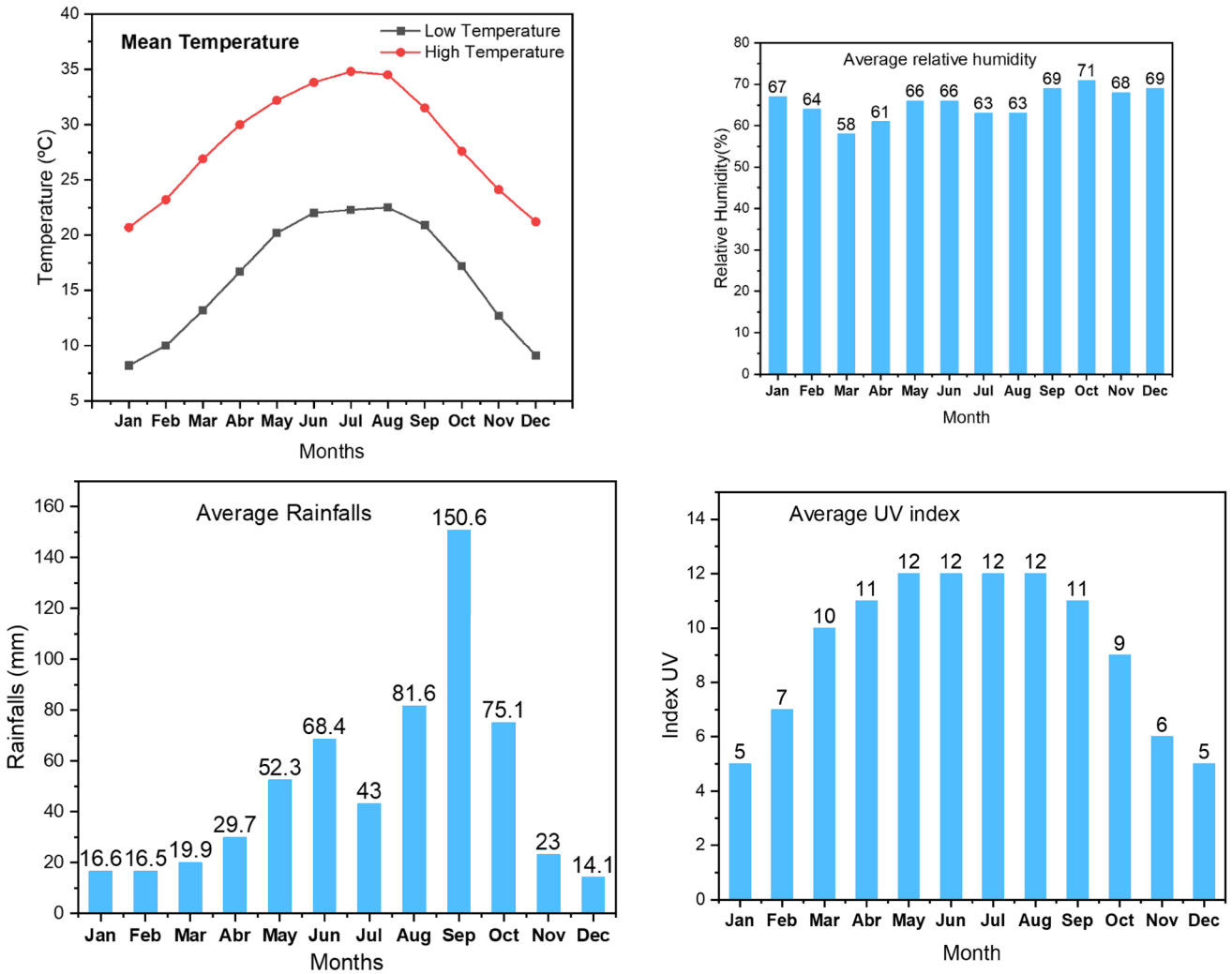

Fig. 4 Top: Average temperature and RH, and bottom: Average of rainfall and UV radiation

3 Results and discussion

The X-ray diffraction pattern (X-RD) of the clay tiles utilized in this study is depicted in Fig. 5. Analysis of the pattern reveals the presence of several crystalline phases, including quartz mineral, hematite, and calcium aluminosilicate.

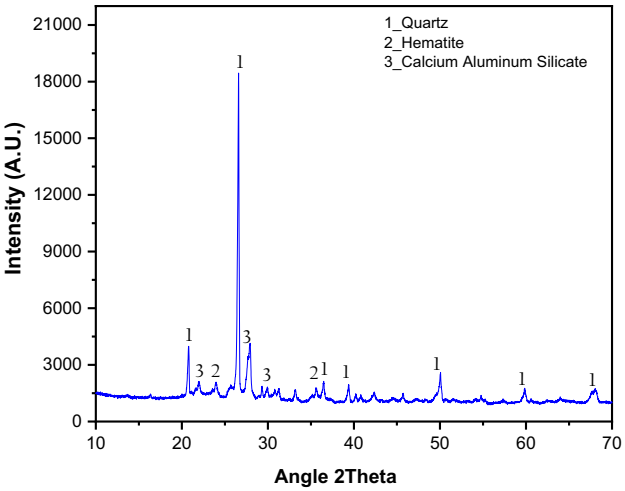

Fig. 5 X-RD pattern for clay tiles

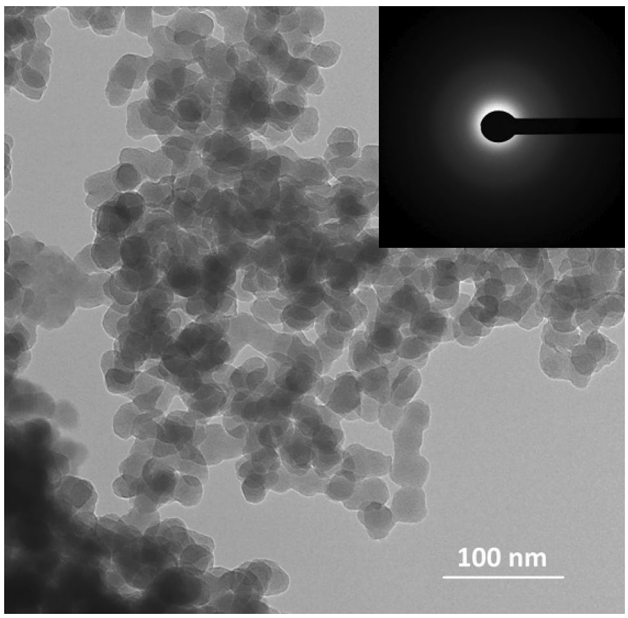

Fig. 6 TEM image of the NS nanoparticles used for T1

As can be seen, there is a high presence of crystallinity in the material, resulting from the transformation of the compounds due to the firing of the clay. The high presence of quartz (SiO_2) promotes a high compatibility with the nanoparticles resulting from the applied treatment.

The morphology of the functionalized nanoparticles, T1 and T2, was evaluated using TEM analysis. As the T1 and T2 nanoparticles exhibited similar morphological characteristics, a single representative image was utilized for the assessment. Figure 6 illustrates that the particles are amorphous in nature, with diameters ranging from approximately 20 to 30 nm. Additionally, it was observed that these nanoparticles tend to form agglomerates in their solid state.

These results confirm the successful synthesis of nanoparticles with sizes below 100 nm. Furthermore, electron diffraction patterns verified the amorphous structure of the synthesized material [35, 43, 44].

The results obtained using the total color differential (ΔE*) technique in the treated and exposed samples are presented in Fig. 7. Two tolerance thresholds for ΔE* are included, as established by ISO 12647–4 and EN 15886:2010 standards. The first threshold is indicated by a dotted line at 3.5, which is considered acceptable or as a minimum perceptible change to the human eye. The second threshold is set at ΔE* > 2 (short dash), indicating an unacceptable and evident change to the human eye. For this study, a change of ΔE* in the range of 2–3 was selected, which could be considered acceptable in materials of historical interest as per EN 16581:2016.

The initial measurements, recorded at 0 M and 0 h, represent the data collected 48 h post-treatment application (REF) and immediately prior to exposure in both media. As illustrated in the graphs presented in Fig. 7, the ΔE* values exhibit

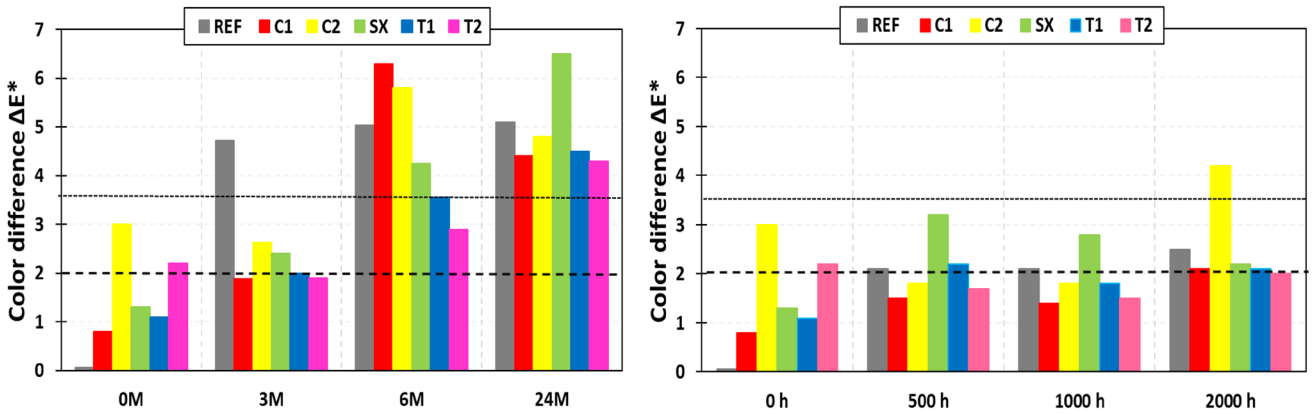

Fig. 7 Total color difference, ΔE*, of fired clay samples exposed to: **a** urban/industrial environment and **b** accelerated QUV

close similarity across all treatments at this stage. Notably, treatments T2 and C2 demonstrate a significant alteration in the visual appearance of the samples, surpassing the threshold at which changes become perceptible to the human eye. The differences observed at this stage can be explained by a temporary damp appearance effect. This effect caused the treated sample surfaces to exhibit an opaque appearance immediately after application. Over time, this opacity lessened and became almost imperceptible to the human eye within a few days. Consequently, subsequent measurements taken at 3 months (3 M) and 500 h (500 h) showed a slight reduction in ΔE* for both treatments under both exposure conditions.

In the case of samples placed in an urban/industrial environment (Fig. 7**a**), it was observed that there was a consistent trend towards an increase in ΔE* with prolonged exposure time. Specifically, samples without treatment exhibited a change exceeding the threshold for materials of historical significance after 3 months, and after 6 months, the change became perceptible to the human eye for REF, C1, and C2 samples. Interestingly, at 24 months of exposure, samples C1 and C2 displayed a decrease in the value of ΔE*, while SX showed an increase above 2. This behavior may be attributed to the deposition of contaminant particles such as dust and volatile organic compounds on the substrate surface, leading to a color change due to a combination of natural weathering and a decrease in surface hydrophobicity [45]. It is worth noting that samples T1 and T2 exhibited only a slight change in appearance, remaining within the maximum threshold ΔE* allowed for buildings of historical significance.

The substantial color variation observed on the surface treated with SX can be attributed to the higher concentration of the active agent (90% siloxanes) in comparison to T1 and T2, where only 20% of this agent was utilized in the production of the functionalized nanoparticles. Previous studies on siloxane-based treatments have indicated that color alterations are noticeable as a result of polymer structure degradation [46]. This deterioration may be induced by biological growth, particle deposition, and the development of crust or light films on surfaces. Consequently, a gradual darkening and significant changes in optical appearance are evident [10, 35, 47].

The impact of artificial weathering on the samples, as depicted in Fig. 7**b**, revealed minimal changes in the ΔE* values compared to those exposed to the natural environment. It is evident that the majority of the samples remained within the threshold of 2 after 2000 h of exposure. This behavior can be attributed to the fact that the samples were only subjected to UV radiation, temperature, and humidity. Consequently, the decline in hydrophobic properties or aging of these treatments is primarily a result of the dissociation of methyl bonds due to continuous interaction with UV radiation [48, 49]. These findings suggest that particles present in the natural environment, such as volatile particles, suspended solids, NOx, and/or SOx, have a more pronounced impact on the optical properties of the substrates developed through different treatments.

The CIELab colorimetry coordinates obtained through Eq. 1 were utilized to digitally simulate the color change in the samples using the Nix Color Sensor software, enabling visualization of the resulting colors. Figure 8 displays the colorimetry data for the specimens both before and after exposure to the environmental conditions outlined in this study.

The results indicate that tiles exposed to an industrial environment display a darker shade, as illustrated in Fig. 8**c**, with a color difference (ΔE*) greater than 2. This change in color is attributed to the deposition of various particles present in urban and industrial settings. Conversely, minimal color change was observed in samples exposed to a controlled environment, as shown in Fig. 8**b**, with color measurements closely resembling those of unexposed samples (Fig. 8**a**). Therefore, it can be confirmed that the color variation in exposed samples is primarily the result of direct contamination from substances such as dust, soot, and other pollutants.

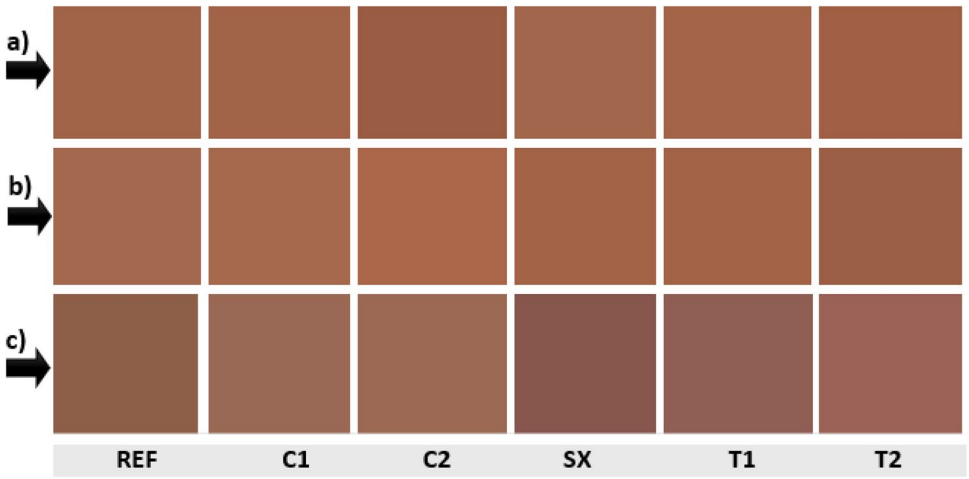

Fig. 8 Colorimetry obtained by digital simulation of clay tiles treated and exposed to: **a** without exposure, **b** 2000 h in a QUV chamber and **c** 24 months in an industrial environment

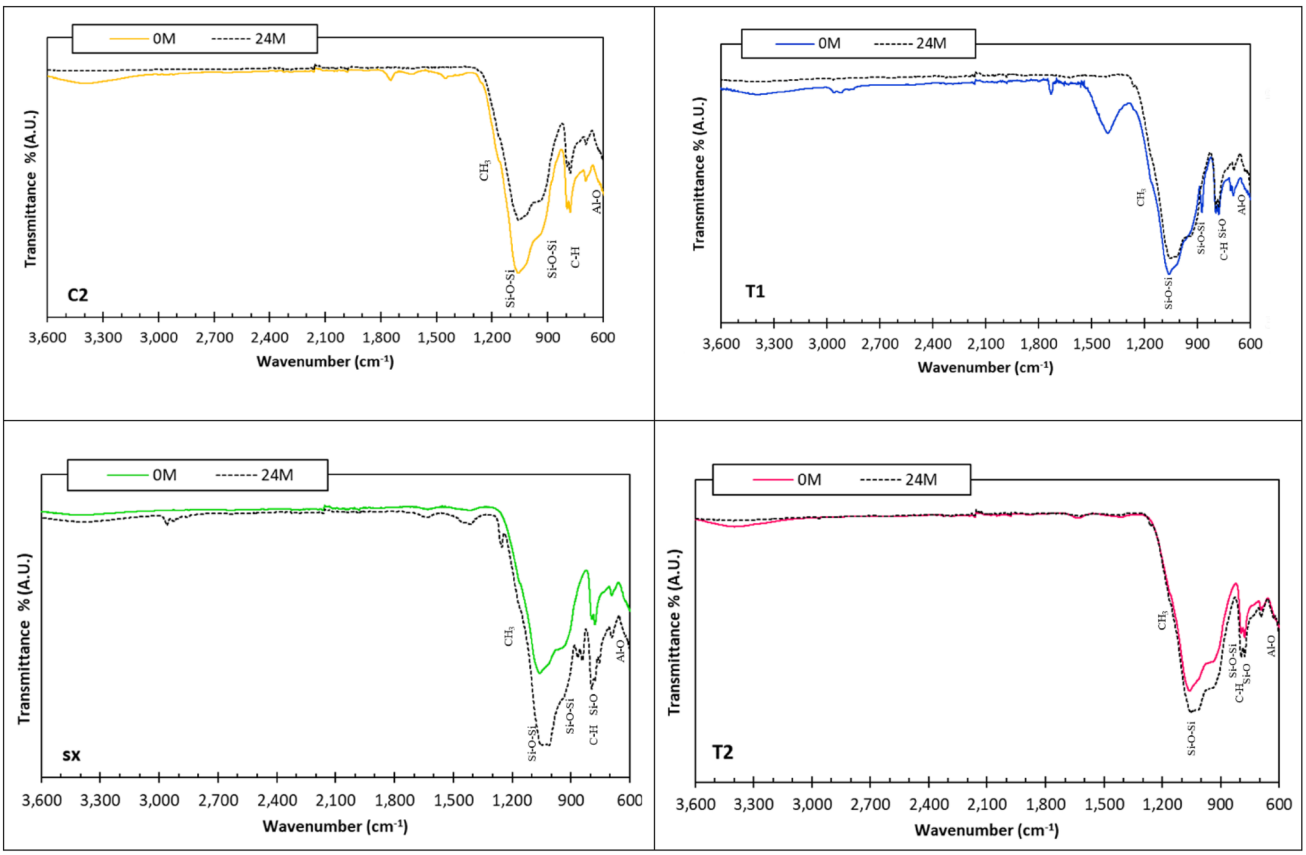

Fig. 9 Infrared spectra of tile samples treated with C2, SX, T1, and T2

The primary cause of aging and subsequent degradation of hydrophobic polymeric surface treatments is the joint interaction between particles present in the atmosphere and weathering. As a result, most of these treatments are unsuitable for outdoor use [45]. It is widely known that organic compounds are susceptible to the dissociation of the base agent polymer chains utilized in the treatments under analysis [48]. In order to evaluate the resistance of these treatments to weathering, the surface of the tiles was examined before and after exposure in different environments using FTIR.

The FTIR spectra obtained in the range of 600–3600 cm^{-1} for samples exposed to an urban/industrial environment were compared to the reference samples (see Fig. 9). The analysis specifically focused on treatments involving the use of water as a dispersant or placement vehicle.

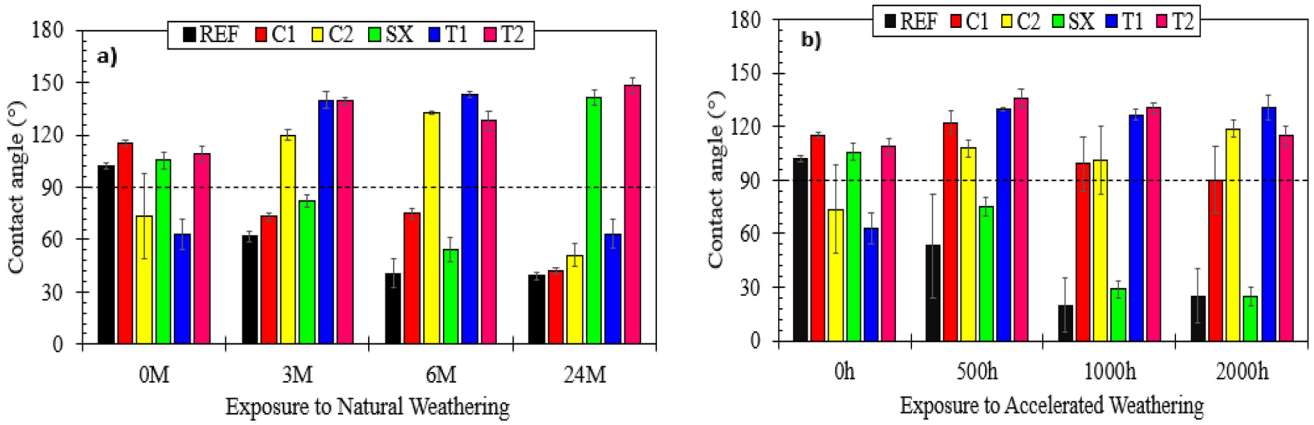

Fig. 10 Contact angle of specimens exposed to: **a** urban/industrial environment and **b** Accelerated QUV

The predominant functional groups of tiles are primarily located within the spectral range of 600–1500 cm^{-1}, which signifies the inherent composition or characteristic features of the base material. This range encompasses polycrystalline and crystalline materials, mainly associated with Si–O and Al-O groups. The broad peaks observed between 1100 and 810 cm^{-1} are linked to the symmetric stretching vibration absorption of Si – O–Si, while the peaks at 780 cm^{-1} correspond to the bending vibrations of Si–O. These findings provide insight into the composition of the clay tile itself or may be a result of initial surface treatments [50]. Furthermore, it is important to note that the characteristic absorption peaks of Al-O are typically found around 625 and 850 cm^{-1} [50, 51]. Based on the analysis, it is evident that secondary signals or those derived from surface treatments may exhibit a lower intensity.

The stretching vibrations observed in the characteristic peaks of the -CH_3 functional groups, which occur at 1210–1255 cm^{-1} and 2950–2970 cm^{-1}, as well as the C-H functional group peak at 810 cm^{-1}, suggest the presence of hydrophobic properties resulting from surface treatment. It is noteworthy that treatments SX and T2 display a more pronounced peak in the 1250–1260 cm^{-1} range, with the 1255 cm^{-1} signal indicating the stable position of -CH_3. This observation supports the sustained hydrophobicity as indicated by contact angle measurements (refer to Fig. 11**b**).

In contrast, treatments C2 and T1 exhibit a decrease in peaks within the 1250–1260 cm^{-1} and 2960 cm^{-1} ranges, indicating a potential breakdown of -CH_3 bonds and a subsequent decline in hydrophobicity. This reduction is further supported by the early loss of hydrophobicity observed in urban/industrial settings for these treatments, likely attributed to the polar-non-polar interactions between OH^- and -CH_3 functional groups. In order to conduct a more thorough chemical analysis in future studies, it is advisable to cross-reference these findings with additional techniques, including X-ray diffraction, as mentioned elsewhere [52].

The results from the contact angle measurements conducted on specimens that were unexposed and those exposed in both urban/industrial and accelerated QUV environments are outlined in Fig. 10**a**, as well as Fig. 10**b**, respectively. In this study, the initial contact angles of the samples were measured and established as the baseline values. Subsequently, samples were collected at specific intervals during the exposure period, including natural environmental conditions over 3 months (M), 6 months, and 24 months, as well as accelerated environmental conditions over 500 h, 1000 h, and 2000 h. It is important to note that the boundary between hydrophilic (contact angle < 90°) and hydrophobic (contact angle > 90°) is represented by the dotted line in the graphs.

The initial results from groups 0 M and 0 h indicate the presence of a hydrophobic surface, with variations of approximately ± 4° for C1, SX, and T4. Additionally, the contact angle resulting from treatments C2 and T1 exhibited fluctuations of around ± 18° for T1 and ± 24° for C2 within the initial 48-h period. These observations can be attributed to the initial interaction of the active agent of treatments with the surface, which subsequently stabilizes over time. Conversely, it was noted that treatments C2, T1, and T2 demonstrated an increasing angle with prolonged exposure time.

The impact of exposure environment on surface treatments is evident in the significant reduction of contact angle observed in samples exposed to urban/industrial settings. This phenomenon is attributed to the combined effect of atmospheric deposition, which interferes with surface hydrophobicity, as noted by Borsoi et al. [53]. Furthermore, ultraviolet radiation-induced photooxidation and degradation of O-CH_3 bonds contribute to adhesion loss, cracking,

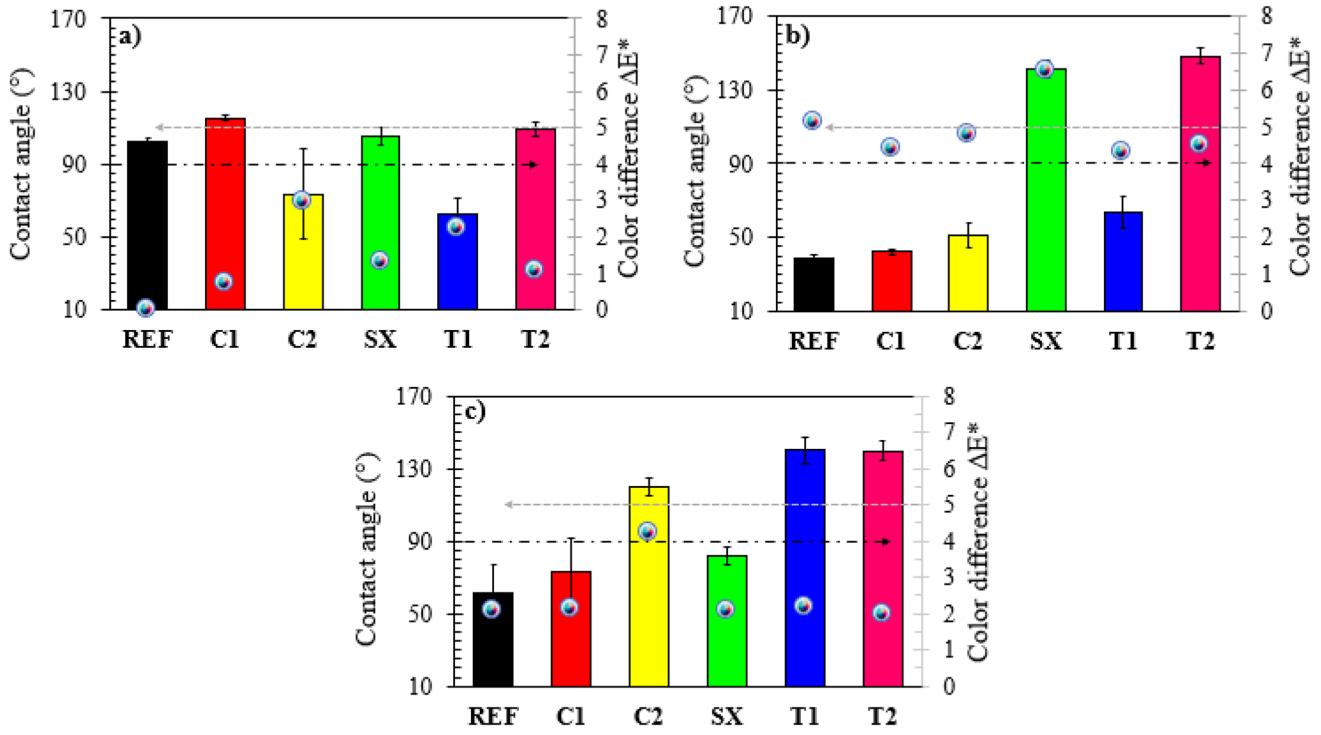

Fig. 11 Contact angle vs colorimetry of specimens: **a** unexposed; and after, **b** 24 months of atmospheric exposure and **c** 2000 h of exposure in QUV

yellowing, and diminished surface brightness. Consequently, the deterioration of this property exposes the substrate to various forms of degradation facilitated by water and external agents.

In contrast, the samples subjected to exposure in a QUV climatic chamber (Fig. 10**b**) demonstrated superior stability of the contact angle in treatments C1, C2, T1, and T2, when compared to treatment SX, which displayed a significant decrease after 500 h of exposure. Treatment SX comprises 90% siloxane, whereas C1 and C2 consist of a combination of siloxanes and silanes, and T1 and T2 contain modified nanoparticles.

Surface treatments with contact angles greater than 90^{0} have been widely demonstrated to provide protection for materials against the ingress of water and harmful agents, including dissolved salts, volatile organic compounds, and biodecay. This protection is achieved by minimizing the entry of moisture [35, 47, 54, 55]. It is important to note that the effectiveness and stability of these treatments are contingent upon the type and quantity of the agent, as well as the specific characteristics of the chain involved. Therefore, the selection of the appropriate treatment is crucial in ensuring the desired level of protection for the material in question.

The permanence of hydrophobicity and the color change of the substrate surface are crucial factors in determining the suitability of surface treatments. In Fig. 11, the relationship between these two parameters is depicted, showing the behavior of the treatments before (Fig. 11**a**) and after the maximum exposure time (Fig. 11**b** for exposure in a natural environment, and Fig. 11c in a controlled QUV environment). The bars in the figure represent the contact angle data obtained, while the circle markers indicate the differential color change recorded.

In the specimens without exposure (as shown in Fig. 8**a**), the ΔE* values ranged from 1 to 3, with C2 and T1 exhibiting the highest values. However, these values were below the threshold perceptible to the human eye (ΔE* < 3.5). These variations can be directly attributed to the formation of a polymeric film by the active ingredients of each treatment, which alters the luminosity (L*) of the substrate and results in a color change that is considered imperceptible to the human eye. Based on the hydrophobic property, only treatments C1, SX, and T2 meet the two acceptance criteria. It is worth noting that the REF specimens (i.e., without treatment) initially exhibited surface hydrophobicity, possibly due to a product applied during the manufacturing process of these tiles. However, this initial behavior changed during exposure, as detailed below.

The impact of natural weathering on color alteration (ΔE*) and contact angle modification is depicted in Fig. 11**b**. Despite the type of treatment, exposure to weathering resulted in a color change exceeding 3.5 and a decrease in

Table 2 Average values of initial and secondary absorption rates

Accelerated weathering (2000 h)	Absorption rate, $\times 10^{-4}$ mm/s$^{1/2}$					
	REF	C1	C2	SX	T1	T2
Initial	299.9	22.1	15.6	250.5	35.1	9.1
Secondary	14.6	24.1	25.9	11.6	9.0	22.4
Natural weathering (6 M)	Absorption rate, $\times 10^{-4}$ mm/s$^{1/2}$					
	REF	C1	C2	SX	T1	T2
Initial	297.9	27.8	12.3	168.0	28.4	16.4
Secondary	15.2	25.6	21.8	10.6	26.3	35.7

contact angle for treatments C1, C2, and T1. Conversely, treatments SX and T2 exhibited an increase in contact angle to approximately 140°. In this context, only treatment T2 would be considered acceptable as it aligns with the specified criteria.

After exposure, it was observed that the initial hydrophobicity of the remaining treatments was not preserved on the surface of the specimens. The ΔE* value, which indicates color change, was.

significantly affected by the deposition and adhesion of atmospheric particles on the surface tiles. Specifically, treatment SX exhibited a ΔE* value of 6.5, which is visibly perceptible and considered undesirable for treatments intended for use in historical heritage. Conversely, treatment T2 demonstrated a lower ΔE* value of 4.5, indicating better maintenance of hydrophobic properties and a resulting surface cleaning effect due to a higher contact angle. The presence of these treatments can lead to two potential outcomes. On one hand, the impact of water droplets during rain can result in a self-cleaning effect as it washes away particles from the surface of the tiles. However, on the other hand, non-hydrophobic surfaces may experience an adhesion effect during precipitation, where water droplets interact with any film formed by treatments, leading to a wet appearance effect on the surface. These opposing outcomes highlight the complex interplay between surface properties and environmental factors, emphasizing the importance of considering these dynamics in surface treatment and maintenance strategies.

Upon analysis, it was noted that treatments C2, T1, and T2 exhibited a notably high contact angle in a controlled environment (Fig. 11**c**), indicating the sustained hydrophobic nature of the specimens surfaces. Additionally, there was a slight increase in color change in these treatments, with the exception of commercial treatment C2 (ΔE* = 4.2). In the specific conditions of the weathering method employed, all treatments satisfied the designated criteria, thus warranting their consideration for application in historical materials. It is important to note, however, that the closed chamber setting with indoor UV radiation, controlled temperature, and elevated humidity did not encompass other environmental factors such as particles or compounds that could potentially interact with the sample surfaces, as would occur in the case of atmospheric exposure.

Based on the results from the two environments utilized in this study, it is evident that a thorough review of the procedures and standards for evaluating various treatments, including the application and types of compounds used, is necessary for materials of historical significance. This review will be crucial in ensuring the appropriate preservation and treatment of such materials in the future.

Upon completion of the exposure period in both controlled and natural environments, noticeable alterations in the hydrophobic properties of the treated specimen surfaces were detected. To assess the efficacy of the treatments in preventing the infiltration of detrimental substances into the matrix of the tiles, the initial water absorption rate of the specimens was determined. This assessment was conducted following 2000 h of exposure in a controlled environment (QUV) and after an approximate equivalent of 6 months (6 M) of natural exposure. It is worth noting that the 2000 h duration corresponds to 4000 h of natural weathering. Table 2 displays the average initial and secondary absorption rates (10^{-4} mm/s$^{1/2}$) for samples subjected to various hydrophobic treatments and exposed to both an accelerated QUV environment (2000 h) and a natural urban/industrial environment (6 M).

A significant reduction in initial absorption rates, ranging from 80 to 90%, was observed across all treatments compared to the reference (REF) in both environments, except for treatment SX. Notably, treatment T2 exhibited an initial absorption rate of 9.1×10^{-4} mm/s$^{1/2}$, representing a substantial decrease of up to 32 times. This behavior is likely attributed to the presence of a protective coating on the sample surface, which effectively maintains its hydrophobic functionality in the exposed environment or results in a reduction of water absorption by over 95%.

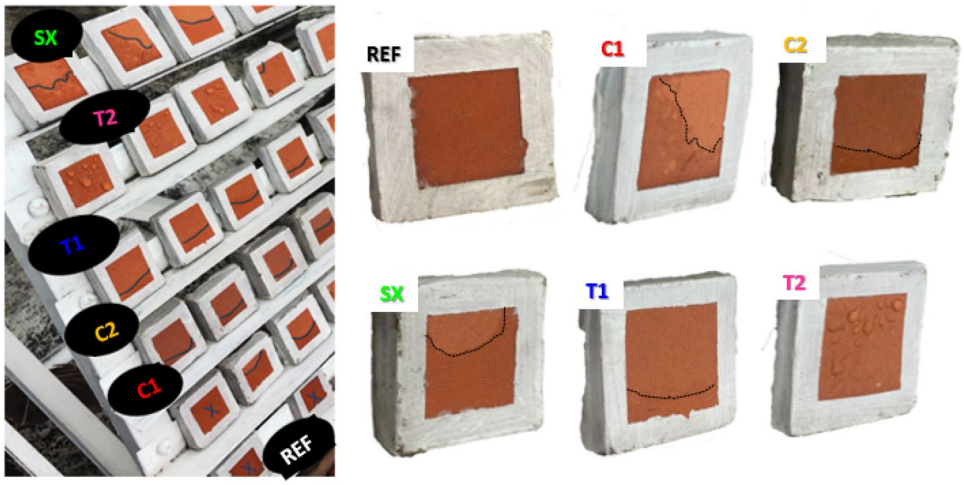

Fig. 12 Images of the specimens of clay tiles in natural exposure after a rainy event

In addition, it is noteworthy that the initial absorption of the samples subjected to SX treatment closely resembled that of the untreated samples, indicating a reduction of 9%. This observation is consistent with existing literature, which suggests that water-repellent treatments, such as siloxane, may not be fully effective for surfaces submerged in water [47].

Based on the results presented in Table 2, certain images have been captured as proof of the exposure to an urban/industrial environment for a period of six months following rainfall (refer to Fig. 12). In order to measure the extent of wetting using ImageJ software, a deliberate dotted white line was applied to the surface to demarcate the boundary between the dry and wet areas. The images indicate a correlation between the observed results and the water absorption rate. Notably, samples REF and SX exhibited a wetting of over 70% of the surface area, while sample C1 showed a wetting of 60%. In contrast, samples C2 and T1 displayed a wetting of approximately 25–30% in the study area. Interestingly, sample T2 demonstrated water droplets adhering to the surface, yet without penetrating the material due to the continued presence of hydrophobic properties.

Based on the findings, it is evident that treatment T2 has demonstrated superior performance across both environmental conditions and weathering methods. In contrast, the other treatments have exhibited a decline in the functionality and longevity of the hydrophobic surface following 6 months of outdoor exposure. Consequently, with regard to their performance, it is advisable to refrain from recommending all treatments except for T2 for current infrastructure or those of historical significance. This recommendation is further underscored by the fact that a substantial portion of the baked clay masonry is utilized for ornamental purposes, with approximately 90% of historically significant infrastructure being constructed using tiles [8]. Therefore, any aesthetically or visibly perceptible alterations would be deemed undesirable for this type of infrastructure.

The application of surface treatments has led to an enhancement in the properties of the tiles, primarily through the reduction of wettability resulting from increased hydrophobicity. This has effectively contributed to the preservation of the original appearance of the tiles. It is important to acknowledge that the effectiveness of these qualities can be compromised by the choice of surface modifier or the quantity of active ingredient applied. Excessive use of such materials can lead to adverse effects, particularly when exposed to weather conditions, resulting in significant color changes due to degradation and/or deterioration. The results suggest that treatment T2 effectively protects this clay material by maintaining its hydrophobic properties against environmental conditions, making it a practical preservation solution. In addition, the application of this hydrophobic surface treatment has the potential to effectively postpone, and in some cases, halt the impact of environmental elements on material substrates. This in turn prolongs their operational lifespan and mitigates the need for premature interventions which may incur unforeseen expenses. Such treatment offers a viable solution to counteract the depreciation of constructed (and/or historical) assets, while simultaneously reducing the excessive use of raw materials needed for the maintenance, repair, or replacement of deteriorated materials. Consequently, it plays a crucial role in fostering a positive attitude towards conservation and promoting sustainable consumption practices.

4 Conclusions

The application and evaluation of various surface treatments on baked clay substrates, following the experimental conditions described in this work, allow us to conclude the following:

1. The exposure to urban/industrial environments resulted in a noticeable darkening and alteration in visual appearance, as indicated by the ΔE* values. This transformation is attributed to the interaction between the water-repellent film and atmospheric agents, leading to surface darkening due to the deposition of atmospheric particles. Notably, treatment SX exhibited the most pronounced visual impact, surpassing the ΔE* threshold of > 2.
2. Despite visual changes, the static contact angle results demonstrated that the hydrophobic properties were retained, with contact angles exceeding 140° for treatments SX and T2. Treatment T2, in particular, showcased a contact angle exceeding 145°, facilitating a self-cleaning effect and significantly reducing water absorption rates, thereby delaying substrate deterioration. Conversely, samples C1, C2, and T1 displayed contact angles below 90°, attributed to the combined effects of atmospheric agents and photo-oxidation.
3. The degradation of O-CH_3 bonds in natural environments has resulted in a loss of adhesion and noticeable color changes on exposed substrates. Analysis using Fourier-transform infrared spectroscopy (FTIR) has confirmed the conversion of -CH_3 groups into C-H or -OH radicals. These chemical changes have been correlated with shifts in colorimetric properties, providing valuable insight into the mechanisms underlying the observed alterations.
4. The performance of surface treatments depends on the affinity and interaction that develops between the substrate and the active ingredient (such as siloxanes, silanes, among others). Therefore, it is important to understand its nature before application on current and/or historical heritage, since the efficiency is based on obtaining and maintaining a contact angle > 90º and ΔE* values < 2, as required for this type of construction material.

Finally, treatment T2 has proven to be a highly effective option for preserving clay materials in both contemporary and historical constructions. Its ability to resist weathering and its stable interaction with the substrate make it a valuable choice for conservation efforts. The hydrophobic properties of T2 are attributed to the surface modification of T1 nanoparticles during synthesis, which results in a composition featuring a mix of OH^- and -CH_3 groups. This composition effectively delays the hydroxylation effect typically observed in hydrophobic treatments, leading to a significant reduction in the rate of water absorption. As a result, harmful agents are prevented from penetrating clay tiles or other clay materials, thereby safeguarding them against physical, chemical, and biological damage. Ultimately, the application of treatment T2 extends the service life of the treated substrate, reducing the need for frequent repairs and interventions in preserved structures.

Acknowledgements Not applicable.

Author contribution D. Cruz-Moreno: Validation, Formal analysis, Writing—Original Draft. M. Neri-Álvarez: Conceptualization, Methodology, Investigation. G. Ortiz-Rabell: Writing—review & editing, Formal analysis. M.A. Neri-Flores: Investigation, Visualization. G. Fajardo-San-Miguel: Funding acquisition, Supervision, Resources, Writing—review & editing.

Funding The research described in this manuscript was funded by CONAHCYT under Agreements CB-2016/285453 and IT1765-21. Mónica Neri-Álvarez thanks CONAHCYT for Scholarship No. 872560 granted for her master's training.

Data availability Yes. Data sets generated during the current study are available from the corresponding author on reasonable request.

Declarations

Ethics approval and consent to participate Not applicable.

Competing interests The authors declare that they have no known competing financial interests or personal relationships that could have appeared to influence the work reported in this paper.

References

1. Saba M, Quiñones-Bolaños EE, Martínez Batista HF. Impact of environmental factors on the deterioration of the Wall of Cartagena de Indias. J Cult Herit. 2019;39:305–13. https://doi.org/10.1016/j.culher.2019.03.001.
2. Bin Tan S, Ti ESW. What is the value of built heritage conservation? Assessing spillover effects of conserving historic sites in Singapore. Land Use Policy. 2020;91:104393. https://doi.org/10.1016/j.landusepol.2019.104393.
3. Tweed C, Sutherland M. Built cultural heritage and sustainable urban development. Landsc Urban Plan. 2007;83:62–9. https://doi.org/10.1016/j.landurbplan.2007.05.008.
4. Sesana E, Gagnon AS, Bonazza A, Hughes JJ. An integrated approach for assessing the vulnerability of world heritage sites to climate change impacts. J Cult Herit. 2020;41:211–24. https://doi.org/10.1016/j.culher.2019.06.013.
5. Ghafari E, Arezoumandi M, Costa H, Júlio E. Influence of nano-silica addition in the durability of UHPC. Constr Build Mater. 2015;94:181–8. https://doi.org/10.1016/j.conbuildmat.2015.07.009.
6. Chithra S, Senthil Kumar SRR, Chinnaraju K. The effect of colloidal nano-silica on workability, mechanical and durability properties of high performance concrete with copper slag as partial fine aggregate. Constr Build Mater. 2016;113:794–804. https://doi.org/10.1016/j.conbuildmat.2016.03.119.
7. Mohseni E, Miyandehi BM, Yang J, Yazdi MA. Single and combined effects of nano-SiO_2, nano-Al_2O_3 and nano-TiO_2 on the mechanical, rheological and durability properties of self-compacting mortar containing fly ash. Constr Build Mater. 2015;84:331–40. https://doi.org/10.1016/j.conbuildmat.2015.03.006.
8. Liu S, Wang R, Yu J, Peng X, Cai Y, Tu B. Effectiveness of the anti-erosion of an MICP coating on the surfaces of ancient clay roof tiles. Constr Build Mater. 2020;243: 118202. https://doi.org/10.1016/j.conbuildmat.2020.118202.
9. Anna LP. Thermal-energy analysis of roof cool clay tiles for application in historic buildings and cities. Sustain Cities Soc. 2015;19:271–80.
10. Joseph E, Junier P. Metabolic processes applied to endangered metal and wood heritage objects: Call a microbial plumber!, N. Biotechnol. 2020;56:21–6. https://doi.org/10.1016/j.nbt.2019.11.003.
11. Elert K, Rodriguez-Navarro C. Degradation and conservation of clay-containing stone: a review. Constr Build Mater. 2022;330: 127226. https://doi.org/10.1016/j.conbuildmat.2022.127226.
12. Nik VM, Mundt-Petersen SO, Kalagasidis AS, De Wilde P. Future moisture loads for building facades in Sweden: climate change and wind-driven rain. Build Environ. 2015;93:362–75. https://doi.org/10.1016/j.buildenv.2015.07.012.
13. Macchia A, Ruffolo SA, Rivaroli L, Malagodi M, Licchelli M, Rovella N, Randazzo L, La Russa MF. Comparative study of protective coatings for the conservation of Urban Art. J Cult Herit. 2020;41:232–7. https://doi.org/10.1016/j.culher.2019.05.001.
14. Wu J, Wu G, Zheng T, Zhang X, Zhou K. Value capture mechanisms, transaction costs, and heritage conservation: A case study of Sanjiangyuan National Park. China, Land Use Policy. 2020;90: 104246. https://doi.org/10.1016/j.landusepol.2019.104246.
15. Hosseini M, Karapanagiotis I. Advanced Materials for the Conservation of Stone. 2018. https://doi.org/10.1007/978-3-319-72260-3.
16. Shaquihuanga Ayala, D. L. (2014). "Evaluación del estado actual de los muros de albañilería confinada en las viviendas del sector Fila Alta-Jaén."
17. Morillas L, et al. Nitrogen supply modulates the effect of changes in drying–rewetting frequency on soil C and N cycling and greenhouse gas exchange. Glob Change Biol. 2015;21(10):3854–63.
18. Brito JD, Pereira C, Silvestre JD, Flores-Colen I. Expert Knowledge-based Inspection Systems Inspection, Diagnosis, and Repair of the Building Envelope. Cham: Springer International Publishing; 2020.
19. Ausset, P., et al. (2000). Past air pollution recordings on stone monuments: The heads of the Kings of Juda statues from Notre-Dame Cathedral (Paris). In: Proceedings of the 9th International Congress on Deterioration and Conservation of Stone, Elsevier.
20. Cully P, Karasu F, Müller L, Jauzein T, Leterrier Y. Self-cleaning and wear-resistant polymer nanocomposite surfaces. Surf Coatings Technol. 2018;348:111–20. https://doi.org/10.1016/j.surfcoat.2018.05.040.
21. Ding X, Zhou S, Gu G, Wu L. A facile and large-area fabrication method of superhydrophobic self-cleaning fluorinated polysiloxane/TiO_2 nanocomposite coatings with long-term durability. J Mater Chem. 2011;21:6161. https://doi.org/10.1039/c0jm04546b.
22. Drugă B, Ukrainczyk N, Weise K, Koenders E, Lackner S. Interaction between wastewater microorganisms and geopolymer or cementitious materials: Biofilm characterization and deterioration characteristics of mortars. Int Biodeterior Biodegrad. 2018;134:58–67. https://doi.org/10.1016/j.ibiod.2018.08.005.
23. Šuligoj A, Štangar UL, Tušar NN. Photocatalytic air-cleaning using TiO2 nanoparticles in porous silica substrate. Chem Pap. 2014;68:1265–72. https://doi.org/10.2478/s11696-014-0553-7.
24. Efome JE, Baghbanzadeh M, Rana D, Matsuura T, Lan CQ. Effects of superhydrophobic SiO2 nanoparticles on the performance of PVDF flat sheet membranes for vacuum membrane distillation. Desalination. 2015;373:47–57. https://doi.org/10.1016/j.desal.2015.07.002.
25. Varshney P, Mohapatra SS. Durable and regenerable superhydrophobic coatings for brass surfaces with excellent self-cleaning and anti-fogging properties prepared by immersion technique. Tribol Int. 2018;123:17–25. https://doi.org/10.1016/j.triboint.2018.02.036.
26. Tricoli A, Righettoni M, Pratsinis SE. Anti-fogging nanofibrous sio2 and nanostructured sio 2-tio2 films made by rapid flame deposition and in situ annealing. Langmuir. 2009;25:12578–84. https://doi.org/10.1021/la901759p.
27. Kim DS, Suh A, Yang S, Yoon DK. Grooving of nanoparticles using sublimable liquid crystal for transparent omniphobic surface. J Colloid Interface Sci. 2018;513:585–91. https://doi.org/10.1016/j.jcis.2017.11.033.
28. Liu M, Hou Y, Li J, Tie L, Guo Z. Transparent slippery liquid-infused nanoparticulate coatings. Chem Eng J. 2018;337:462–70. https://doi.org/10.1016/j.cej.2017.12.118.

29. García O, Malaga K. Definition of the procedure to determine the suitability and durability of an anti-graffiti product for application on cultural heritage porous materials. J Cult Herit. 2012;13:77–82. https://doi.org/10.1016/j.culher.2011.07.004.
30. Borhani-Esfahani S, et al. An environmentally friendly titania–silica core–shell nanoparticles coating for protection of tiled facade of cultural-historical buildings. Res Surfaces Interfaces. 2021;2: 100004.
31. Kouroutzi M, et al. Application of TiO_2 nanoparticles in clay roofing tiles as a photocatalytic active material. Mater Proceed. 2022;5(1):90.
32. Ferri L, Lottici, et al. Study of silica nanoparticles – polysiloxane hydrophobic treatments for stone-based monument protection. J Cult Herit. 2011;12:356–63.
33. Kapridaki C, et al. TiO_2–SiO_2–PDMS nano-composite hydrophobic coating with self-cleaning properties for marble protection. Progr Organ Coat. 2013;76:400–10.
34. Liu, Q., et al. (2013). Effects of surface energies of biomimetic materials for stone conservation on reinforcement properties. Herit. Sci. 20.
35. Cruz-Moreno D, Fajardo G, Flores-Vivian I, Orozco-Cruz R, Ramos-Rivera C. Applied Surface Science Multifunctional surfaces of portland cement-based materials developed with functionalized silicon-based nanoparticles. Appl Surf Sci. 2020;531: 147355. https://doi.org/10.1016/j.apsusc.2020.147355.
36. Lakshmi RV, Bharathidasan T, Bera P, Basu BJ. Fabrication of superhydrophobic and oleophobic sol-gel nanocomposite coating. Surf Coatings Technol. 2012;206:3888–94. https://doi.org/10.1016/j.surfcoat.2012.03.044.
37. Oliveira MLS, Flores EMM, Dotto GL, Neckel A, Silva LFO. Nanomineralogy of mortars and ceramics from the Forum of Caesar and Nerva (Rome, Italy): The protagonist of black crusts produced on historic buildings. J Clean Prod. 2021;278: 123982. https://doi.org/10.1016/j.jclepro.2020.123982.
38. Facio DS, Mosquera MJ. Simple strategy for producing superhydrophobic nanocomposite coatings in situ on a building substrate. ACS Appl Mater Interfaces. 2013;5(15):7517–26.
39. Chelazzi D, Baglioni P. From nanoparticles to gels: A breakthrough in art conservation science. Langmuir. 2023;39(31):10744–55.
40. Olivieri F, et al. Mesoporous silica nanoparticles as carriers of active agents for smart anticorrosive organic coatings: a critical review. Nanoscale. 2021;13(20):9091–111.
41. Olivieri F, et al. Innovative silver-based capping system for mesoporous silica nanocarriers able to exploit a twofold anticorrosive mechanism in composite polymer coatings: tailoring benzotriazole release and capturing chloride ions. ACS Appl Mater Interfaces. 2021;13(40):48141–52.
42. Fajardo G, Cruz-López A, Cruz-Moreno D, Valdez P, Torres G, Zanella R. Innovative application of silicon nanoparticles (SN): Improvement of the barrier effect in hardened Portland cement-based materials. Constr Build Mater. 2015;76:158–67. https://doi.org/10.1016/j.conbuildmat.2014.11.054.
43. She W, Yang J, Hong J, Sun D, Mu S, Miao C. Superhydrophobic concrete with enhanced mechanical robustness: Nanohybrid composites, strengthen mechanism and durability evaluation. Constr Build Mater. 2020;247: 118563. https://doi.org/10.1016/j.conbuildmat.2020.118563.
44. Wu G, Liu D, Chen J, Liu G, Kong Z. Preparation and properties of super hydrophobic films from siloxane-modified two-component waterborne polyurethane and hydrophobic nano SiO2. Prog Org Coat. 2019;127:80–7. https://doi.org/10.1016/j.porgcoat.2018.06.016.
45. Orlowsky J, Braun F, Groh M. The influence of 30 years outdoor weathering on the durability of hydrophobic agents applied on obernkirchener sandstones. Buildings. 2020. https://doi.org/10.3390/buildings10010018.
46. Ingrosso C, et al. UV-curable nanocomposite based on methacrylic-siloxane resin and surface-modified TiO_2 nanocrystals. ACS Appl Mater Interfaces. 2015;7(28):15494–505.
47. Pan X, Shi Z, Shi C, Ling TC, Li N. A review on surface treatment for concrete – Part 2: Performance. Constr Build Mater. 2017;133:81–90. https://doi.org/10.1016/j.conbuildmat.2016.11.128.
48. Yu F, Gao J, Liu C, Chen Y, Zhong G, Hodges C, Chen M, Zhang H. Preparation and UV aging of nano-SiO2/fluorinated polyacrylate polyurethane hydrophobic composite coating. Prog Org Coatings. 2020;141: 105556. https://doi.org/10.1016/j.porgcoat.2020.105556.
49. Oliveira MLS, Tutikian BF, Milanes C, Silva LFO. Atmospheric contaminations and bad conservation effects in Roman mosaics and mortars of Italica. J Clean Prod. 2020;248: 119250. https://doi.org/10.1016/j.jclepro.2019.119250.
50. Lavat AE, Trezza MA, Poggi M. Characterization of ceramic roof tile wastes as pozzolanic admixture. Waste Manag. 2009;29:1666–74. https://doi.org/10.1016/j.wasman.2008.10.019.
51. Piskin S, Figen AK, Ozkan E, Ozcay U. Structural characterization of seydisehir red mud to utilization in roof tile manufacturing. IFAC Proc. 2013;15:484–7. https://doi.org/10.3182/20130825-4-US-2038.00010.
52. Occhipinti R, et al. Chemical and colorimetric analysis for the characterization of degradation forms and surface colour modification of building stone materials. Constr Build Mater. 2021;302: 124356.
53. Borsoi G, Esteves C, Flores-Colen I. Effect of hygrothermal aging on hydrophobic treatments applied to building exterior claddings. Coatings. 2020;10:363.
54. Beirami K, Baghshahi S, Ardestani M, Riahi N. Synthesis and characterization of hydrophobic nano-silica thin coatings for outdoor insulators. Process Appl Ceram. 2020;14:40–6. https://doi.org/10.2298/PAC2001040B.
55. Kua HW, Gupta S, Aday AN, Srubar WV. Biochar-immobilized bacteria and superabsorbent polymers enable self-healing of fiber-reinforced concrete after multiple damage cycles. Cem Concr Compos. 2019;100:35–52. https://doi.org/10.1016/j.cemconcomp.2019.03.017.